

# Needleless Electrospinning: Developments and Performances

Haitao Niu<sup>1</sup>, Xungai Wang<sup>1,2</sup> and Tong Lin<sup>1</sup>

<sup>1</sup>Centre for Material and Fibre Innovation, Deakin University, Geelong

<sup>2</sup>School of Textile Science and Engineering, Wuhan Textile University

<sup>1</sup>Australia

<sup>2</sup>China

## 1. Introduction

Electrospinning technique has attracted a lot of interests recently, although it was invented in as early as 1934 by Anton (Anton, 1934). A basic electrospinning setup normally comprises a high voltage power supply, a syringe needle connected to power supply, and a counter-electrode collector as shown in Fig. 1. During electrospinning, a high electric voltage is applied to the polymer solution, which highly electrifies the solution droplet at the needle tip (Li & Xia, 2004). As a result, the solution droplet at the needle tip receives electric forces, drawing itself toward the opposite electrode, thus deforming into a conical shape (also known as “Taylor cone” (Taylor, 1969)). When the electric force overcomes the surface tension of the polymer solution, the polymer solution ejects off the tip of the “Taylor cone” to form a polymer jet. The charged jet is stretched by the strong electric force into a fine filament. Randomly deposited dry fibers can be obtained on the collector due to the evaporation of solvent in the filament. There are many factors affecting the electrospinning process and fiber properties, including polymer materials (*e.g.* polymer structure, molecular weight, solubility), solvent (*e.g.* boiling point, dielectric properties), solution properties (*e.g.* viscosity, concentration, conductivity, surface tension), operating conditions (*e.g.* applied voltage, collecting distance, flow rate), and ambient environment (*e.g.* temperature, gas environment, humidity).

Electrospun nanofibers exhibit many unique characteristics, such as high surface-to-mass ratio, high porosity with excellent pore interconnectivity, flexibility with reasonable strength, extensive selection of polymer materials, ability to incorporate other materials (*e.g.* chemicals, polymers, biomaterials and nanoparticles) into nanofibers through electrospinning, and ability to control secondary structures of nanofibers in order to prepare nanofibers with core/sheath structure, side-by-side structure, hollow nanofibers and nanofibers with porous structure (Chronakis, 2005). These characteristics enable electrospun nanofibers to find applications in filtrations, affinity membranes, recovery of metal ions, tissue engineering scaffolds, release control, catalyst and enzyme carriers, sensors and energy storage (Fang *et al.*, 2008). In spite of the wide applications, electrospun nanofibers are produced at a low production rate when conventional needle electrospinning setup is used, which hinders their commercialization. Electrospinning

with large scale nanofiber production ability has been explored, and some inspiring results have been achieved. This chapter summarizes the recent research progress in large scale electrospinning technologies.

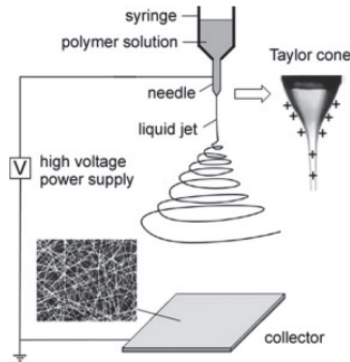


Fig. 1. Schematic illustration of a basic electrospinning setup, the Taylor cone, and a SEM image of electrospun nanofibers (Li & Xia, 2004).

## 2. Downward multi-jet electrospinning

A straightforward way to increase the electrospinning throughput is to use multi-jet spinnerets as shown in Fig. 2a. The fiber productivity can be simply increased by increasing the jet number (Varesano *et al.*, 2009, 2010; Yang *et al.*, 2010). However, multi-jet electrospinning has shown strong repulsion among the jets and this may lead to reduced fiber production rate and poor fiber quality, which is the main obstacle to practical application. To reduce the jet repulsion, jets have to be set at an appropriate distance, and a large space is required to accommodate the needles for the mass nanofiber production.

To stabilize and optimize the electrospinning process an extra-cylindrical electrode has been used as an auxiliary electrode to cover the multi-jet spinneret (Kim *et al.*, 2006). As shown in Fig. 2b, the presence of the external electrode dramatically reduces the fiber deposition area, thus improving the fiber production rate. Nevertheless, coarser fibers were observed, because the auxiliary electrode shortened the chaotic motion of multi-jets in electrospinning.

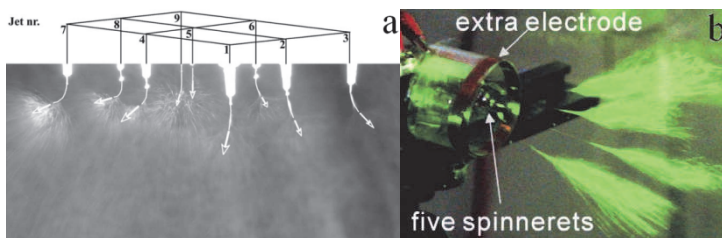


Fig. 2. (a) A multi-jet electrospinning setup (Theron *et al.*, 2005), (b) multi-jet electrospinning with a cylindrical auxiliary electrode (Kim *et al.*, 2006).

In electrospinning, the ejected solution jet carries a large amount of charges, which drive the jet stretching and fiber deposition on the collector. According to the electrospinning mechanism, it can be deduced that interferences in multi-jet electrospinning are unable to be eliminated completely, which will be a barrier to the industrialization of multi-jet electrospinning. Furthermore, the successful operation of multi-jet electrospinning requires a regular cleaning system to avoid the blockage of the needle nozzles. Setting the cleaning device for each needle makes it almost impossible to use multi-jet electrospinning for mass production of nanofibers.

In addition to the multi-jet electrospinning, porous tubes have also been used as electrospinning spinnerets to improve the fiber productivity. This system is herein still classified into multi-jet electrospinning because the electrospinning process is based on conveying solutions inside the tube channels. A porous polyethylene tube with a vertical axis was used to electrospin nanofibers (Fig. 3a) (Dosunmu *et al.*, 2006). The production rate was reported to be 250 times greater than that of single needle electrospinning. However, the SEM results of obtained nanofibers showed large variations in the fiber diameter.

In another example of tube electrospinning (horizontal tube), the polymer solution was pushed through the tube wall with many holes at 1 ~ 2 kPa pressure (Fig. 3b) (Varabhas *et al.*, 2008). This setup can only produce 0.3 ~ 0.5 g/hr of nanofibers due to the small number of holes (fiber generators) that can be drilled per unit area. Although it was mentioned that the production rates can be easily scaled up by increasing the tube length and the number of holes, the space between holes can't be reduced much because of the electric field repulsion between the jets. The strong jet interference in this setup can even result in nanofiber belt instead of fiber web (Varabhas *et al.*, 2008).

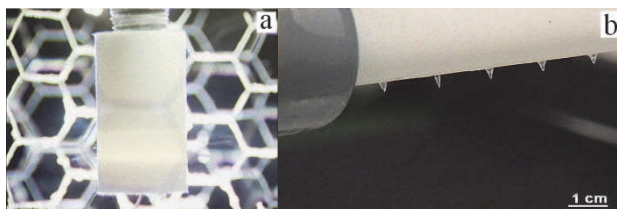


Fig. 3. (a) Electrospinning using a vertical tubular foam spinneret (Dosunmu *et al.*, 2006), (b) horizontal tube electrospinning (Varabhas *et al.*, 2008).

Wang *et al.* reported a conical wire coil electrospinning spinneret, which can work at up to 70 kV without causing corona discharges (Wang *et al.*, 2009). As shown in Fig. 4a~c, the spinning solution was held in the wire cone without using any solution channels. Due to the large surface tension and visco-elasticity, the polymer solution can be retained inside the wire cone. When a high electric voltage was applied to the wire coil, solution was stretched out from the wire surface and the gap between wires to form solution jets. Without using defined solution channels, the fiber ejected independently, eliminating the limitation of jet number that was formed in multi-jet electrospinning and tube electrospinning. In comparison with conventional needle electrospinning, wire coil electrospinning can improve the electrospinning throughput noticeably and produce nanofibers with smaller fiber diameter (Fig. 4d). The results also indicated that fibers prepared by coil electrospinning had a wider diameter distribution than those produced by the needle electrospinning.

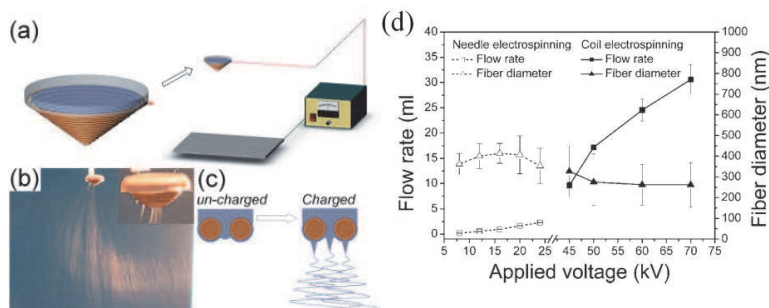


Fig. 4. (a) Schematic illustration of conical wire coil electrospinning setup, (b) photograph of the electrospinning process, (c) illustration of jet formation, (d) comparison between needle electrospinning and coil electrospinning (PVA concentration = 9 wt%; collecting distance = 15 cm) (Wang *et al.*, 2009).

An edge-plate electrospinning setup for improving the fiber productivity was reported by Thoppey *et al* (Thoppey *et al.*, 2010). A plate (Angle with respect to horizontal  $\theta = 40^\circ$ ) for retaining solution was used as a spinneret to electrospin polyethylene oxide (PEO) nanofibers (Fig. 5a). In this method an electrically insulated reservoir connected with one or more plastic pipettes supplied solution to the charged plate, and each pipette supplied a solution stream as jet initiation site. It was found that the production rate was increased by over 5 times even using a single spinning site (one pipette) without getting coarser fibers and wider diameter distribution (Fig. 5 b & c). The surface tension of polymer solution plays a vital role, and the plate angle must be set appropriately according to the solution properties, otherwise solution dripping may occur.

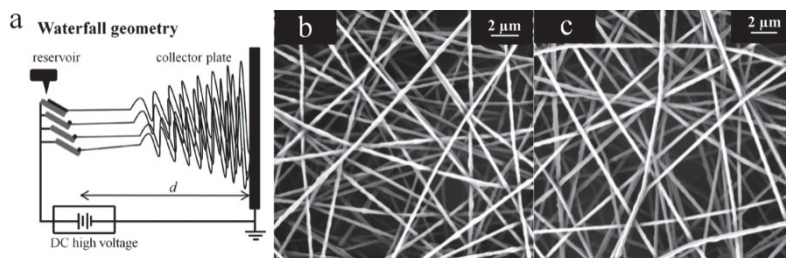


Fig. 5. (a) Schematic illustration of plate edge electrospinning, (b) & (c) SEM images of nanofibers electrospun from (b) conventional needle electrospinning (collecting distance = 15 cm, applied voltage = 11 kV) and (c) edge-plate geometry (collecting distance = 35 cm, applied voltage = 28 kV) (Thoppey *et al.*, 2010).

In another electrospinning design, a solution reservoir was used to provide spinning solution to a metal roller electrospinning spinneret (Fig. 6) (Tang *et al.*, 2010). The polymer solution droplets were splashed onto the surface of a metal roller by a solution distributor, which had a hole at the bottom. When the voltage was applied, solution droplets adhering on the surface of metal roller spinneret were ejected and stretched under the electric force to form nanofibers. This setup was proposed to have the ability to perform electrospinning with improved fiber production rate.

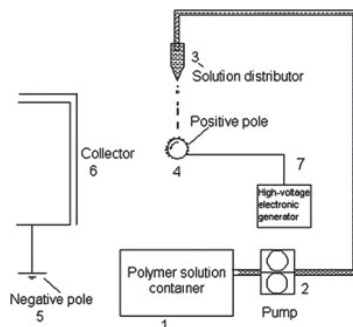


Fig. 6. Schematic illustration of splashing electrospinning setup (Tang *et al.*, 2010).

A rotary cone was used as electrospinning spinneret to perform electrospinning recently, which used a glass pipe to supply the PVP solution to the cone to ensure enough solution for continuous electrospinning (Fig. 7a) (Lu *et al.*, 2010). The electrospinning throughput of this setup was reported to be 1000 times larger than that of conventional needle electrospinning. The morphologies of nanofibers prepared by the cone electrospinning were nearly the same as those produced by conventional needle electrospinning (Fig. 7 b&c).

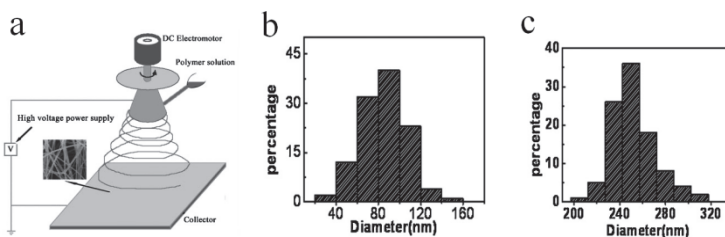


Fig. 7. (a) Schematic illustration of the rotary cone electrospinning setup (inset: SEM image of collected PVP nanofibers, rotational speed of cone = 100 rpm, applied voltage = 30 kV, collecting distance = 20 cm, solution throughput = 10 g min<sup>-1</sup>), (b) fiber diameter distribution of needle electrospinning, (c) fiber diameter distribution of rotary cone electrospinning (Lu *et al.*, 2010).

### 3. Upward needleless electrospinning

#### 3.1 Electrospinning techniques

A good electrospinning method suitable for manufacturing nanofibers should have minimal dependences on the fluidic channel numbers to improve the fiber productivity. It should be universal for processing polymer solutions of different properties. Some upward needleless electrospinning setups have good potential.

Yarin and Zussman (Yarin & Zussman, 2004) reported a two-layer-fluid electrospinning setup (Fig. 8a) that could dispose of the problems related to multi-jet electrospinning. In this setup, the lower fluid layer was a ferromagnetic suspension and the upper layer was the polymer solution to be spun. During electrospinning, when a normal magnetic field was applied to the system, steady vertical spikes were formed perturbing the interlayer interface. As a result of applying a high voltage to the fluid at the same time, thousands of jetting ejected upward (Fig.

8b). This upward electrospinning system required a complicated setup and the resultant nanofibers had large fiber diameter and wide diameter distribution (Fig. 8c).

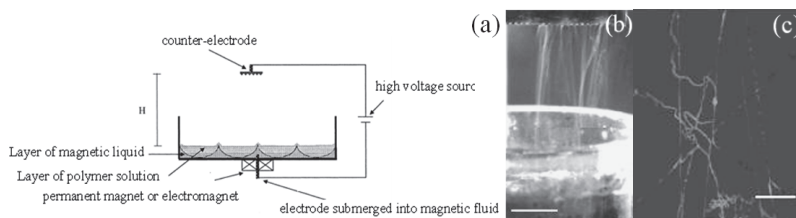


Fig. 8. (a) A two-layer-fluid electrospinning setup, (b) multiple jets ejected toward the counter-electrode, (c) an image of as-spun fibers (scale bar is 50 mm) (Yarin & Zussman, 2004).

In another upward electrospinning work, bubbles or humps were generated on the free surface of a polymer solution to initiate the electrospinning process (Liu et al., 2008). Unlike the previous design, a high pressure gas was used by inserting a gas tube to the bottom of the solution reservoir. A flat aluminum plate was used as collector above the solution. When a high voltage was applied to the solution, Taylor cones were easily formed from the humps. The fiber production rate was reported to depend on the gas pressure, the solution properties and the applied voltage. However, fibers prepared by this method contained large beads.

Jirsak *et al.* (Jirsak *et al.*, 2005) invented a needleless electrospinning setup by using a rotating roller as the nanofiber generator. When the roller was partially immersed into a polymer solution and slowly rotates, the polymer solution was loaded onto the upper roller surface. Upon applying a high voltage to the electrospinning system, an enormous number of solution jets can be generated from the roller surface upward (Fig. 9). This setup has been commercialized by Elmarco Co with the brand name “Nanospider™”.

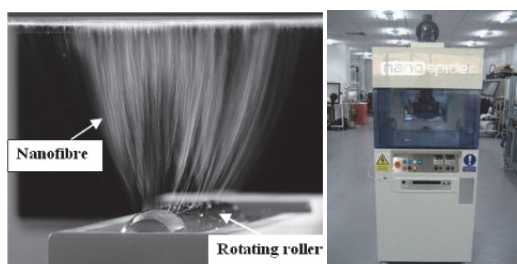


Fig. 9. Roller electrospinning process (left), and commercialized Nanospider™ (right) (Jirsak *et al.*, 2005).

Lukas *et al.* (Lukas *et al.*, 2008) developed a one-dimensional electrohydrodynamic theory to describe the electrospinning of conductive liquids from an open flat surface based on the phenomenon that nanofibers can be electrospun from linear clefts even without being aided by a magnetic fluid underneath (Fig. 10). This work added a general approach toward studying dynamics of surface waves. During electrospinning from a free liquid surface, due to the electric force the amplitude of a characteristic wavelength boundlessly grew faster than the others. The fastest growing stationary wave marked the onset of electrospinning

from a free liquid surface with its jets originating from the wave crests. The proposed theory predicated the critical values of the phenomenon, the critical field strength and corresponding critical inter-jet distance, and the inter-jet distance for field strengths above the critical value. The theory also predicted relaxation time necessary for spontaneous jetting after a high voltage was applied, and explained the fundamental of upward needleless electrospinning.

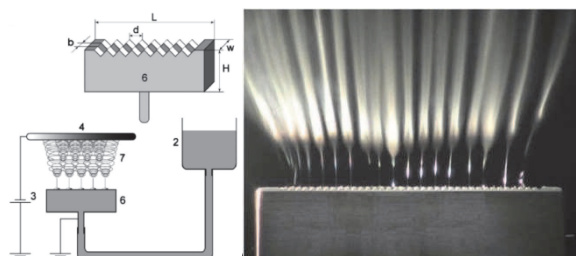


Fig. 10. Schematic illustration of a linear cleft electrospinning setup (left) and electrospinning process (right) (Lukas *et al.*, 2008).

Needleless electrospinning process with rotating spinneret can be summarized as that, the rotation of spinneret loads a thin layer of polymer solution onto the spinneret surface. The rotation and perturbation create conical spikes on the surface of this solution layer. When a high voltage is applied to the spinneret, these spikes tend to concentrate charges and amplify the perturbation and the fluid around the spikes is drawn to these spikes under high electric force. Taylor cones are thus formed. Fine solution jets are then ejected from the tips of these Taylor cones, when the electric force is large enough.

Using a similar design, Niu *et al* systematically compared the needleless electrospinning using different rotary fiber-generators (disc, cylinder or ball) (Niu *et al.*, 2009) (Fig. 11). When PVA solution was charged with a high electric voltage via a copper wire inside the solution vessel, numerous jets/filaments were generated from the spinneret, which deposited on the collector (*e.g.* rotating drum). With the rotation of the spinneret, PVA solution was loaded onto the spinneret surface constantly, leading to continuous generation of polymer jets/filaments. They also used finite element method to analyze electric field and examine the influence of spinneret shape on the electric field profile. They found that the spinneret with a highly concentrated and evenly distributed electric field is the key to efficient needleless electrospinning of uniform nanofibers.

Based on this understanding, a new needleless electrospinning system using a spiral coil wire as fiber generator was invented (Lin *et al.*, 2010). As shown in Fig. 11, when the applied voltage exceeded a critical value, numerous polymer jets were generated from the wire surface. It was also found that the spiral coil had higher fiber production rate than cylinder spinneret of the same dimension, and the fiber diameter was finer with a narrower diameter distribution (Wang *et al.*, 2009).

High throughput production of nanofibers in the name of "Tip-less Electrospinning" (TLES) has been demonstrated by Wu *et al* (Wu *et al.*, 2010), using a circular cylinder as the fiber generator. This is also an upward needleless electrospinning system using rotating spinneret. The solution ejecting process from the generator surface is shown in Fig. 12. Experimental results showed that the yield of poly(ethylene oxide) nanofibers can be more than 260 times in weight compared to that of a single-jet electrospinning.

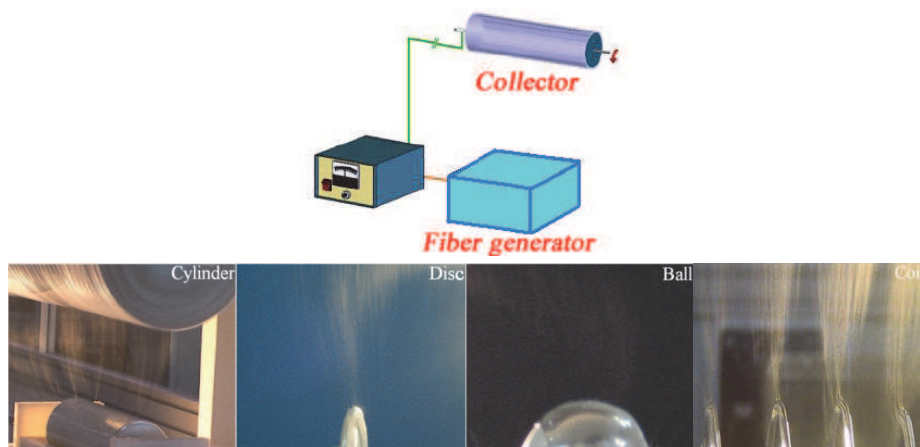


Fig. 11. Schematic illustrations of needleless electrospinning setup, and cylinder, disc, ball, and spiral coil electrospinning processes (Niu *et al.*, 2009; Lin *et al.*, 2010).

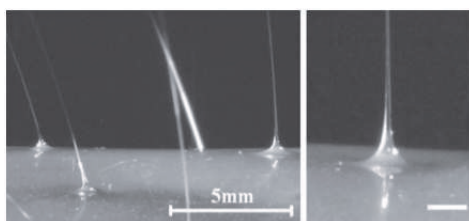


Fig. 12. Fiber ejecting process of a cylinder electrospinning (applied voltage = 70 kV, collecting distance = 15 cm, cylinder diameter = 3 cm) (Wu *et al.*, 2010).

There are significant differences between the needle and upward needleless electrospinning processes. In the upward needleless electrospinning, Taylor cones are created on the surface of polymer solution. If the Taylor cone is stable, it will move together with the surface of rotating roller and produces a solution jet under the strong electric field. Therefore, there must be strong inter-molecular interactions among polymer macromolecules in the solution to stabilize the Taylor cone given that Taylor cone is stretched into a fine jet and deposited on the collector as solid fibers. Different to the conventional needle electrospinning in which Taylor cone is generated and stabilized through constantly feeding polymer solution through the needle, the upward needleless electrospinning forms its Taylor cones by sucking up the solution covering the surrounding fiber generator (Cengiz & Jirsak, 2009). It was observed that the base diameter of Taylor cone in cylinder electrospinning reduced from 1.2 mm to 0.3 mm in the beginning and the end of the electrospinning, respectively (initial polymer film thickness = 1 mm). If the film thickness is further reduced, no Taylor cones or nanofibers can be generated (Wu *et al.*, 2010). Therefore, the solution must have a suitable rheological property. Furthermore, a higher electric voltage is required to initiate the needleless electrospinning, because Taylor cone is formed due to the wave fluctuation.

## 3.2 Parameters affecting needleless electrospinning

### 3.2.1 Applied voltage

Applied voltage is a very important parameter affecting both the electrospinning process and fiber properties. A high applied voltage (usually over 40 kV) is usually required to initiate an upward needleless electrospinning. The critical voltage required to initiate electrospinning is closely related to the material properties, ambient environment (e.g. humidity, temperature) and collecting distance. High critical voltages are required when either the solution concentration or the collecting distance increases (Fig. 13 a & b). This can be explained that at a high concentration solution, the increased viscosity requires a larger electric force to create Taylor cones. Increasing the collecting distance reduces the electric field strength in the electrospinning zone. It was also found that a solution film in the thickness range of 0.5 mm ~ 2 mm was in favor of forming Taylor cones, and could reduce the critical voltage (Fig. 13c) (Wu et al., 2010).

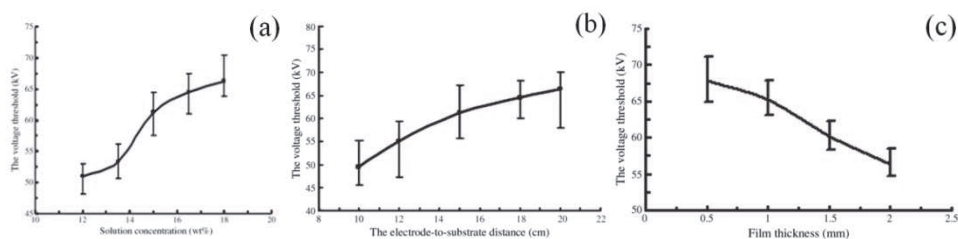


Fig. 13. Critical voltage versus (a) solution concentration (film thickness = 1 mm, electrode-to-substrate distance = 15 cm), (b) electrode-to-substrate distance (film thickness = 1 mm, electrode-to-substrate distance = 15 cm, and polymer solution = 15 wt%), and (c) film thickness (electrode-to-substrate distance = 15 cm and polymer solution = 15 wt%) (Wu et al., 2010).

The spinneret geometry also affects the critical voltage. The spinneret that can generate an intensified electric field (disc spinneret) requires a lower voltage to initiate electrospinning. Niu *et al* found that disc spinneret and cylinder spinneret had different critical voltages for initiating electrospinning, 42 kV and 47 kV, respectively. For the cylinder spinneret at a low applied voltage, the jets were only generated from two end areas, and no jets/filaments were produced from the middle cylinder surface until the applied voltage was above 57 kV. Further increasing the applied voltage led to the generation of jets from the entire cylinder surface. The disc can easily generate high intensity electric field. This was why the disc generated nanofibers regardless of the applied voltage value, as long as the voltage was above the critical value. The fiber morphology was mainly affected by polymer concentration, but little by applied voltage.

Niu *et al* also found that increasing the applied voltage from 47 to 62 kV had little effect on the average fiber diameter in both disc and cylinder electrospinning systems. For the disc electrospinning, the fiber diameter distribution became narrower when the applied voltage was increased (Fig. 14a). For the cylinder electrospinning, the average fiber diameter and

diameter distribution showed a very small dependence on the applied voltage. The applied voltage affected the fiber productivity significantly. The electrospinning throughput in both electrospinning systems increased with the increase in applied voltage. When the applied voltage was increased from 57 kV to 62 kV, the fiber productivities of the cylinder electrospinning and disc electrospinning were very similar, indicating that disc spinneret is a high efficiency fiber generator, although the cylinder spinneret is 100 times longer than the disc spinneret (Fig. 14b).

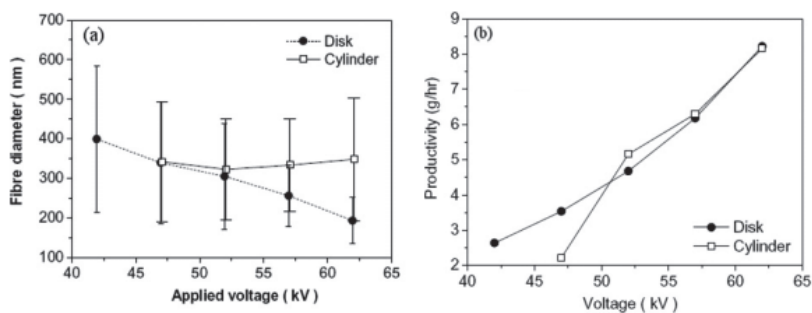


Fig. 14. Influences of applied voltage on (a) fiber diameter, and (b) fiber productivity (collecting distance = 13 cm, PVA concentration = 9 wt%, cylinder diameter = 80 mm, cylinder rim radius = 2 mm, disc diameter = 80 mm, disc thickness = 2 mm) (Niu *et al.*, 2009).

Using a spiral coil, the productivity of electrospun PVA nanofibers increased with the applied voltage (45 kV ~ 60 kV) (Wang *et al.*, 2009). The trends that the fiber diameter decreased but the production rate increased with increasing applied voltage were also reported by other researchers using different polymer systems (Wu *et al.*, 2010). All these results suggest that the applied voltage plays a key role in improving the fiber production rate in the upward needleless electrospinning.

### 3.2.2 Collecting distance

Reducing the fiber collecting distance has a similar effect to increasing the applied voltage, but the collecting distance can't be reduced infinitely. To collect solid nanofibers, the collecting distance must be large enough to ensure sufficient solvent evaporation from the jet before deposition. The minimal collecting distance is dependent on the solution property and the geometry of fiber generator. For example, the minimal collecting distance for the PEO solution was 10 cm when humidity and temperature are 43% RH and 22 °C, respectively (Wu *et al.*, 2010), and 11 cm for the PVA solution (Niu *et al.*, 2009). However, the collecting distance should not be too large either, since a larger distance would require a higher applied voltage to initiate electrospinning, which may cause corona discharge. A good balance should be maintained between the applied voltage and the collecting distance for successful upward needleless electrospinning.

### 3.2.3 Rotating speed of fiber generator

The rotating speed of fiber generator in upward needleless electrospinning may be varied over a wide range, which has an influence on electrospinning. A rotating speed of 40 rpm was reported in two studies (Niu *et al.*, 2009, Wang *et al.*, 2009). Cengiz and Jirsak used 3.2~4 rpm for their designs (Cengiz & Jirsak, 2009, Jirsak *et al.*, 2010). Cengiz *et al.* (Cengiz *et al.*, 2009) found that the fiber diameter decreased when the rotating speed of a cylinder fiber generator (8 cm in length and 2 cm in diameter) was increased. It is normally believed that increasing rotating speed reduces the life span of the Taylor cone. Very fast spinneret rotating speed is not good for improving the fiber productivity.

### 3.2.4 Polymer concentration

The polymer solution concentration plays a vital role in upward needleless electrospinning. When the polymer solution concentration is too low, polymer beads rather than nanofibers are usually produced. When the concentration is very high, the polymer solution becomes too thick to be stretched into jets. As long as polymer solutions can be electrospun into nanofibers successfully, the polymer concentration doesn't affect the fiber diameter significantly.

Niu *et al.* have studied the effect of PVA concentration on needleless electrospinning. They found that when PVA concentration changed from 8 wt% to 11 wt%, fiber diameter did not change significantly. The nanofibers spun from the disc spinneret had a much narrower diameter distribution than those from the cylinder spinneret. However, the electrospinning throughput was highly dependent on the solution concentration. When the PVA concentration was in the range of 8.0 ~ 11.0 wt%, the productivity of disc electrospinning increased with increasing PVA concentration, while the cylinder electrospinning was highly affected by the PVA concentration. When 9 wt% PVA solution was electrospun with an applied voltage of 52 kV, nanofibers were generated from the whole cylinder surface. 9 wt% PVA also gave the largest electrospinning throughput (Fig. 15). Higher PVA concentration resulted in generation of nanofibers only from cylinder ends.

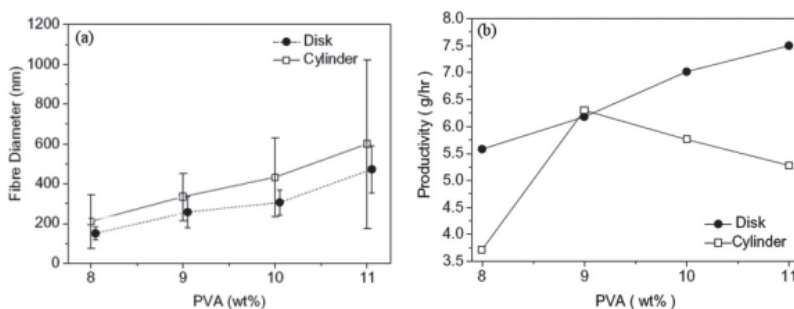


Fig. 15. Influence of PVA concentration on (a) fiber diameter, and (b) fiber productivity (collecting distance = 13 cm, applied voltage = 57 kV, cylinder diameter = 80 mm, cylinder rim radius = 2 mm, disc diameter = 80 mm, disc thickness = 2 mm) (Niu *et al.*, 2009).

The upward needleless electrospinning has good capability of producing nanofibers from different polymer solution systems. In addition to water solvent system, organic solvent systems, *e.g.* dimethylformamide (DMF), have already been used to prepare nanofibers. The polyimide precursor (polyamic acid) produced from 4, 4'-oxydiphthalic anhydride and 4, 4'-oxydianiline in DMF has been electrospun into nanofibers, on a polypropylene spunbond supporting web, with diameters in the range 143 ~ 470 nm using roller electrospinning (Jirsak *et al.*, 2010). Consequently, these polyamic acid fibers can be heated to convert to polyimide nanofibers. Another example is the polyurethane (PU) nanofibers electrospun using the roller electrospinning from PU/DMF solution (Cengiz & Jirsak, 2009).

Chain entanglements and molecular weight are two important properties that can affect the electrospinning process. Shenoy *et al* (Shenoy *et al.*, 2005) reported that the macromolecule chain entanglement characterized by the entanglement number in solution  $(n_e)_{\text{soln}}$  can ultimately determine the formation of beads or fibers. Beads are formed when  $(n_e)_{\text{soln}}$  is below 2 and fibers are produced when  $(n_e)_{\text{soln}}$  is over 2.5. It was found that the PVA with a molecular weight of 67.000 was not spinnable, while other solutions (molecular weight: 80.000 and 150.000) could be successfully electrospun into nanofibers (Cengiz *et al.*, 2009a). The electrospinning throughputs of both PVA solutions increased with increasing PVA concentration (Fig. 16).

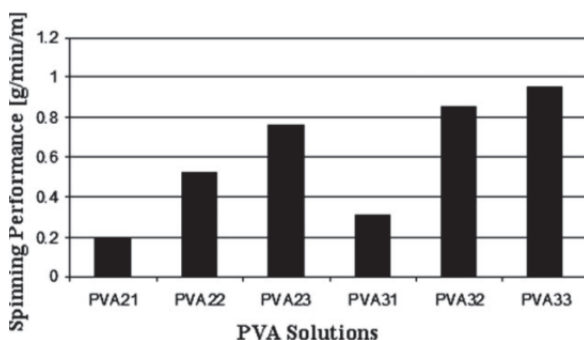


Fig. 16. Influence of polymer solution on the electrospinning performance (cylinder length = 14 cm, cylinder diameter = 2 cm, cylinder rotating speed = 3.2 rpm, collecting distance = 11 cm, applied voltage = 81.2 kV) (Cengiz *et al.*, 2009a).

The addition of salt to the solution can increase the charge density of the solution and improve the electrospinning process. With low or no tetraethylammoniumbromide (TEAB) salt, the PU solution can't be electrospun into nanofibers. When a small amount of TEAB was added into polyurethane solution, the electrospinning was significantly improved. Both fiber diameter and productivity increased with the increase in the TEAB concentration (Cengiz & Jirsak, 2009). The reason for this is that TEAB increases the electric conductivity resulting in the improvement in electrospinning ability.

The upward needleless electrospinning possesses many advantages over the conventional needle electrospinning process. The conglomeration of dopants in the electrospinning solution

can easily block the needle spinneret and cease the electrospinning process. In the absence of capillary spinneret, there will be no nozzle blockage in the needleless electrospinning. PVA nanofibers containing carbon nanotubes (CNTs) have been successfully prepared using a roller electrospinning process (Kostakova *et al.*, 2009).

It was also found that the spinneret geometry significantly affected the electrospinning process and fiber property (Fig. 17). Under the same electrospinning conditions, the disc produced the finest nanofibers with the narrowest fiber diameter distribution. Cylinders produced coarse nanofibers with the largest fiber productivity. Compared to disc and cylinder spinnerets, ball spinneret produced coarser nanofibers with lower productivity. The spiral coil electrospinning combined the advantages of cylinder and disc spinnerets, by producing fine and uniform nanofibers at a high productivity (Lin *et al.*, 2010).

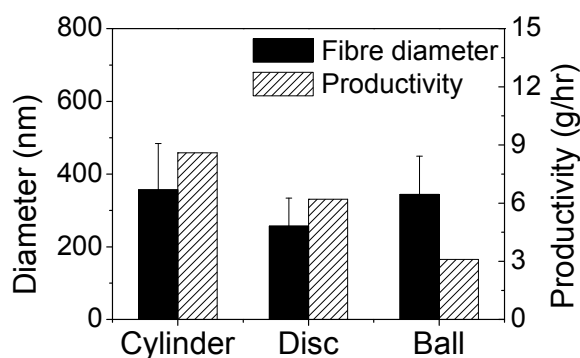


Fig. 17. Comparisons among cylinder, disc and ball spinnerets in fiber diameter and productivity (applied voltage = 57 kV, collecting distance = 13 cm, cylinder diameter = 80 mm, cylinder rim radius = 5 mm, disc diameter = 80 mm, disc thickness = 2 mm, ball diameter = 80 mm).

#### 4. Fiber collection in upward needleless electrospinning

The fiber collection in needleless electrospinning can generally be classified into three types: grounded plate, rotating drum and moving substrate. The plate collector is normally used for electrospinning at a moderately high production rate, *e.g.* multi-jet electrospinning and wire coil electrospinning. However, these fiber collectors are not suitable for upward needleless electrospinning systems, because the deposition of numerous nanofibers accumulates a large amount of charges on the collector, which can finally disturb or even stop the electrospinning process if they are not dissipated quickly. Moving collectors are therefore necessary in these systems. There are two types of moving collectors: rotating drum collector and moving substrate. The drum collector was used by Niu *et al* (Fig. 11).

Drum collector can also collect aligned nanofiber mat. When the mat reaches a certain thickness, it can be peeled off from the collector. Jirsak *et al* (Jirsak *et al.*, 2010) used a moving substrate to collect nanofibers in their systems. The advantage of this type of fiber collection is that nanofibers can be collected continuously and the nanofiber web does not have to be very strong; such a collection system also allows the incorporation of nanofibers into the fiber collecting substrate itself, if required.

## 5. Electric field analysis

One of the vital conditions for initiating an electrospinning process is the high electric field intensity and the strong interactions between electric field and polymer fluid. The electric force has been identified as the driving force for electrospinning. Although the driving force in all electrospinning is the same, the electrospinning process could be influenced by the spinneret geometry. In needle electrospinning, only the polymer solution at the needle tip is under electric force. Induced by a high electric voltage, charges accumulate on a liquid surface, giving rise to electric forces. At a low applied voltage, under the influences of electric force, the droplet reduces its size so that the force balance is maintained. With an increase in the applied voltage, the shape of solution droplet evolves from the hemi-sphere to a cone shape (Taylor cone) with a high electric force concentrated at the tip of the Taylor cone. When the electric field reaches a critical value, the droplet at the cone tip overcomes its surface tension, to eject into the electric field formed between the tip and collector, and a solution jet is thus generated. Through the above analysis, one can conclude that jet initiation is determined by the applied voltage. In needle electrospinning, the critical applied voltage for electrospinning was proposed in equation (1) (Taylor, 1969):

$$V_c^2 = 4 \ln \left( \frac{2h}{R} \right) (1.3\pi R \gamma) (0.09) \quad (1)$$

where  $h$  is the distance from the needle tip to the collector,  $R$  denotes the needle outer radius, and  $\gamma$  is the surface tension. The factor 0.09 was inserted to predict the voltage. Ludas *et al* (Lukas *et al.*, 2008) have explained the self-organization of jets happening on a free liquid surface in needleless electrospinning process. The critical electric field intensity for electrospinning nanofibers was proposed as:

$$E_c = \sqrt[4]{4\gamma\rho g/\epsilon^2} \quad (2)$$

where  $\rho$  is liquid mass density,  $g$  is gravity acceleration,  $\gamma$  is surface tension,  $\epsilon$  is the permittivity. In both the models, electric force plays a crucial role in the jet initiation. In a static electric field, it is well known that the relationship between voltage and electric field intensity can be expressed as:

$$E = -\nabla V \quad (3)$$

Therefore, a surface with a higher curvature will have higher electric field intensity. In needleless electrospinning, because the surface electric field is highly determined by the spinneret shape, the electrospinning process is also influenced by the shape of the spinneret. The region with higher surface curvature can generate high intensity electric field, and electrospinning can therefore be initiated easily from this region.

The electric field of needleless electrospinning spinneret is quite different from needle spinneret. The electric fields of coil-wire and needle electrospinning spinnerets were calculated and compared to examine the relationship between electric field intensity and electrospinning performance (Wang et al., 2009). The intensified electric field is generated on the wire surface (Fig. 18 a & b), the needle spinneret generates intensified electric field at its tip, but with a lower intensity due to the lower applied voltage used (Fig. 18 c & d). This should be the reason as to why a coil-wire electrospinning can produce finer PVA nanofibers than a needle electrospinning (Wang et al., 2009).

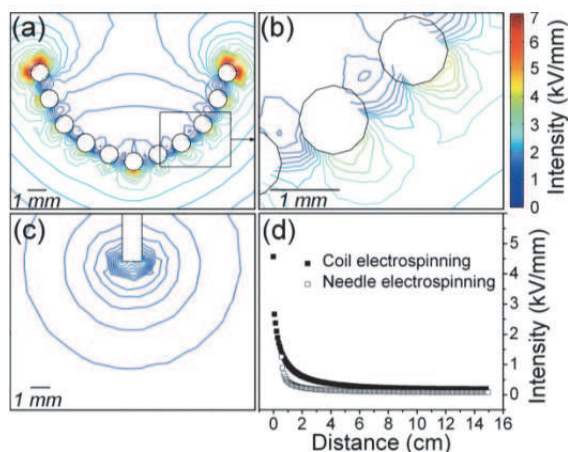


Fig. 18. Cross-sectional view of electric field intensity profiles on (a) & (b) conical coil spinneret (applied voltage = 60 kV), (c) needle spinneret (applied voltage = 22 kV), and (d) electric field intensity profiles along the electrospinning direction. Spinneret (0, 0), collector (0, 15) (Wang et al., 2009).

In the plate edge electrospinning, the sharp edge can generate strong electric field close to the edge, which decays rapidly toward to the ground, while the electric field profile is similar to that of a needle spinneret (Fig. 19 a & b). Many spinning sites can be formed along the entire edge, generating much more solution jets than employing an array of needles (Thoppey *et al.*, 2010). In the plate stack spinneret, more spinning sites can still be formed along these plate edges for generating more nanofibers, although the electric field intensity gradient close to the plate edge is reduced (Fig. 19 c).

Our recent study indicated that the difference in geometry between the cylinder, disc, ball, and coil spinnerets led to totally different electric field intensity profiles. As shown in Fig. 20, much higher electric field intensity is formed at the cylinder top ends than the middle top surface. As a result, the cylinder ends produced nanofibers more easily than the middle area and the nanofibers produced from the whole cylinder had a wide diameter distribution. If the rim radius of the cylinder ends was reduced, stronger electric field tended to be generated. However the electric field in the cylinder middle area was little affected by the rim radius. When the rim radius was 5 mm, the cylinder spinneret resulted in the highest production rate, while the cylinder length and diameter remained unchanged.

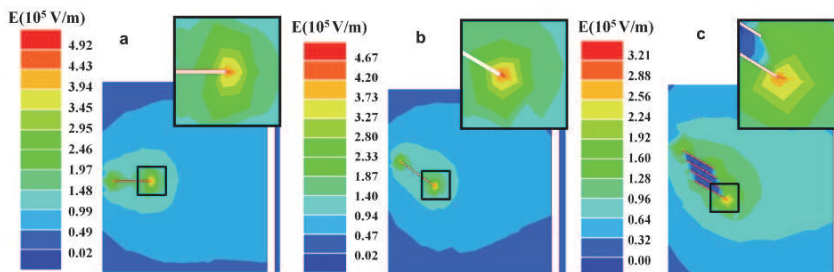


Fig. 19. Electric field intensity distribution of different electrospinning setups (collecting distance = 15 cm, applied voltage = 15 kV, insets are the magnifications of the indicated square areas in each figure), (a) conventional needle electrospinning, (b) edge-plate electrospinning, and (c) waterfall electrospinning (Thoppey *et al.*, 2010).

When the cylinder length and the rim radius were kept unchanged, the area with high electric field intensity shrank with reducing cylinder diameter, and the electric field intensity in the middle surface increased with a decrease in the cylinder diameter (Fig. 20a). Reducing cylinder diameter can contribute to the improvement in electrospinning throughput. It was also reported that when cylinder diameter increased from 1 cm to 6 cm, the critical voltage for electrospinning a PEO solution increased from about 25 kV to 61 kV (Wu *et al.*, 2010).

Cylinders can produce nanofibers from the whole surface, but only when the applied voltage is high enough. This makes the cylinders less efficient compared with other spinnerets such as disc and spring coil, in terms of power consumption. The electric field is narrowly distributed on the disc top edge in Fig. 20b, and the intensity around the disc surface shows a high dependence on the disc thickness. Thinner disc produced higher electric field intensity around the disc circumference. Compared with the cylinders, discs required a lower critical voltage to initiate the electrospinning and produced fibers with a narrower fiber diameter distribution. The thinnest disc showed the largest fiber productivity.

High electric field intensity is mainly generated on the top half of the ball spinneret (Fig. 20c). The generated electric field was more evenly distributed along the ball surface compared to the cylinder spinnerets but had lower intensity. The experimental results also verified the theoretical calculation results that ball spinneret had low production rate and required a higher voltage to initiate electrospinning (Fig. 20c).

The coil spinneret can generate intensified electric field on each spiral. The coil length, coil distance, coil diameter, and wire diameter all showed significant influence on the generated electric field and electrospinning throughput. The electric field intensity decreased with the increase in coil length, thus less polymer jets were produced on each spiral. When the coil distance decreased from 8 cm to 1 cm, the productivity on each spiral decreased gradually since the electric field intensity decreased evidently. The spirals interfered each other when the pitch was too small (*e.g.* 2 cm), very strong electric field was formed on the side area of the coil but much weaker field in the center. The electric field intensity increased with increasing coil diameter, which increased the fiber productivity. The electric intensity increased with the decrease in wire diameter, and the productivity increased slightly. When wire diameter was higher than 6.35 mm, very low electric field intensity was formed, resulting in an evident drop in fiber productivity.

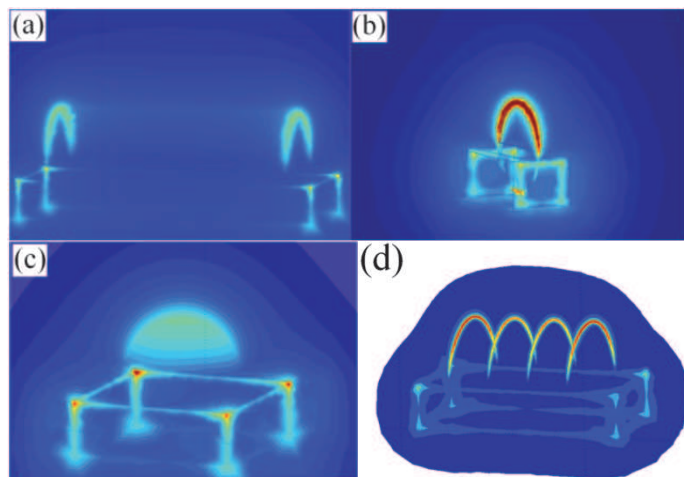


Fig. 20. Electric field intensity profile of (a) cylinder, (b) disc, (c) ball, and (d) coil spinnerets (Lin *et al.*, 2010).

## 6. Issues associated with needleless electrospinning

The upward needleless electrospinning has been proven to be the most successful needleless electrospinning system. The solution bath is normally open to air. The evaporation of solvent from solution can increase the solution viscosity and decrease the solution uniformity. To ensure good electrospinning ability, the solution in the bath must be calculated precisely.

Due to the formation of a large number of solution jets in a small space (from the spinneret to the collector), the concentration of organic solvent in the electrospinning zone could reach a high value during electrospinning. How to recycle the organic solvent efficiently has become a major issue in designing an upward needleless electrospinning system. An air ventilating system has been used to address this issue in the Nanospider™ (Fig. 21).

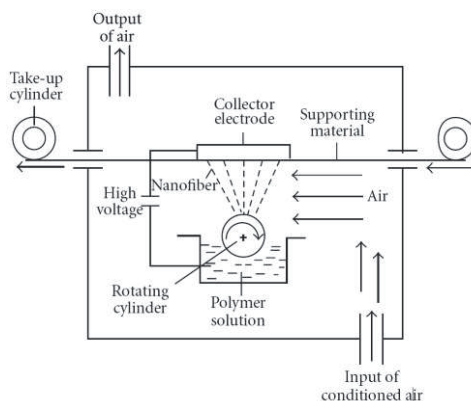


Fig. 21. Air ventilating system used in Nanospider™ (Jirsak *et al.* 2010).

## 7. Concluding remarks

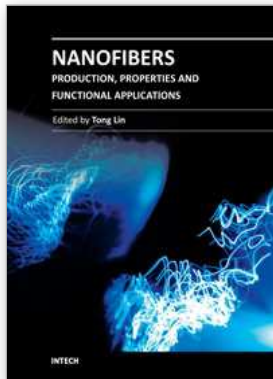
Electrospun nanofibers have numerous applications in various fields. Developing an electrospinning technique for large-scale nanofiber production has become more and more important, as the conventional needle electrospinning has limited productivity and is only suitable for research purpose. Upward needleless electrospinning has been shown the ability to mass produce nanofibers and it is also the most successful design for practical applications. It is expected that the solvent can be recycled effectively so that the fibers are produced with minimal impact on the environment. An efficient needleless electrospinning system to produce nanofibers from thermoplastic polymers is yet to be developed.

## 8. References

- Anton F. (1934). Process and apparatus for preparing artificial threads. *United States patent application 1975504*.
- Cengiz F., Dao T. A. & Jirsak O. (2009). Influence of solution properties on the roller electrospinning of poly(vinyl alcohol). *Polymer Engineering & Science*, Vol. 50, No. 5, (May 2010), pp. 936-43, ISSN 1548-2634
- Cengiz F. & Jirsak O. (2009). The effect of salt on the roller electrospinning of polyurethane nanofibers. *Fibers and Polymers*, Vol. 10, No. 2, pp. 177-84, ISSN 1229-9197
- Cengiz F., Krucinska I., Gliscinska E., Chrzanowski M. & Goktepe F. (2009). Comparative Analysis of Various Electrospinning Methods of Nanofiber Formation. *FIBERS & TEXTILES in Eastern Europe*, Vol. 1, No. 72, (January/March 2009), pp. 13-19.
- Chronakis I. S. (2005). Novel nanocomposites and nanoceramics based on polymer nanofibers using electrospinning process - A review. *Journal of Materials Processing Technology*, Vol. 167, No. 2-3, (August 2005), pp. 283-93, ISSN 0924-0136
- Dosunmu O. O., Chase G. G., Kataphinan W. & Reneker D. H. (2006). Electrospinning of polymer nanofibers from multiple jets on a porous tubular surface. *Nanotechnology*, Vol. 17, No. 4, pp. 1123-27, ISSN 1361-6528
- Fang J., Niu H., Lin T. & Wang X. G. (2008). Applications of electrospun nanofibers. *Chinese Science Bulletin*, Vol. 53, No. 15, pp. 2265-86, ISSN 1001-6538
- Jirsak O., Sanetrik F., Lukas D., Kotek V., Martinova L. & Chaloupek J. (2005). A method of nanofibers production from a polymer solution using electrostatic spinning and a device for carrying out the method. *WO 2005/024101 A1*.
- Jirsak O., Sysel P., Sanetrik F., Hruza J. & Chaloupek J. (2010). Polyamic acid nanofibers produced by needleless electrospinning. *Journal of Nanomaterials*, Vol. 2010, pp. 1-7, ISSN 1687-4110
- Kim G., Choa Y. S. & Kim W. D. (2006). Stability analysis for multi-jets electrospinning process modified with a cylindrical electrode. *European Polymer Journal*, Vol. 42, No. 9, (September 2006), pp. 2031-38, ISSN 0014-3057
- Kostakova E., Meszaros L. & Gregr J. (2009). Composite nanofibers produced by modified needleless electrospinning. *Materials Letters*, Vol. 63, No. 28, (November 2009), pp. 2419-22, ISSN 0167-577X
- Li D. & Xia Y. 2004. Electrospinning of Nanofibers: Reinventing the Wheel? *Advanced Materials*, Vol. 16, No. 14, (July 2004), pp. 1151-70, ISSN 1521-4095
- Lin T., Wang X., Wang X. & Niu H. (2010). Electrostatic spinning assembly. *WO/2010/043002*

- Liu Y., He J. H. & Yu J. Y. (2008). Bubble-electrospinning: a novel method for making nanofibers. *Journal of Physics: Conference Series*, Vol. 96, pp. 012001, ISSN 1742-6596
- Lu B., Wang Y., Liu Y., Duan H., Zhou J., Zhang Z., Li X., Wang W., Lan W. & Xie E. (2010). Superhigh-Throughput Needleless Electrospinning Using a Rotary Cone as Spinneret. *Small*, Vol. 6, No. 15, (August 2010), pp. 1612-16, ISSN 1613-6829
- Lukas D., Sarkar A. & Pokorny P. (2008). Self-organization of jets in electrospinning from free liquid surface: A generalized approach. *Journal of Applied Physics*, Vol. 103, No.8, pp. 084309, ISSN 0021-8979
- Niu H., Lin T. & Wang X. (2009). Needleless electrospinning. I. A comparison of cylinder and disk nozzles. *Journal of Applied Polymer Science*, Vol. 114, No. 6, (December 2009), pp. 3524-30, ISSN 1097-4628
- Shenoy S. L., Bates W. D., Frisch H. L. & Wnek G E (2005). Role of chain entanglements on fiber formation during electrospinning of polymer solutions: good solvent, non-specific polymer-polymer interaction limit. *Polymer*, Vol. 46, No. 10, (April 2005), pp. 3372-84, ISSN 0032-3861
- Tang S., Zeng Y. & Wang X. (2010). Splashing needleless electrospinning of nanofibers. *Polymer Engineering & Science*, Vol. 50, No. 11, (November 2010), pp. 2252-57, ISSN 1548-2634
- Taylor G. (1964). Disintegration of Water Drops in an Electric Field. *Proceedings of the Royal Society of London. Series A. Mathematical and Physical Sciences*, Vol. 280, No. 1382, (July 1964), pp. 383-97, ISSN 1471-2946
- Taylor G. (1969). Electrically driven jets. *Proceedings of the Royal Society of London. Series A, Mathematical and Physical Sciences*, Vol. 313, No. 1515, (December 1969), pp. 453-75, ISSN 1471-2946
- Theron S. A., Yarin A. L., Zussman E. & Kroll E. (2005). Multiple jets in electrospinning: experiment and modeling. *Polymer*, Vol. 46, No. 9, (April 2005), pp. 2889-99, ISSN 0032-3861
- Thoppey N. M., Bochinski J. R., Clarke L. I. & Gorga R. E. (2010). Unconfined fluid electrospun into high quality nanofibers from a plate edge. *Polymer*, Vol. 51, No. 21, (October 2010), pp. 4928-36, ISSN 0032-3861
- Varabhas J. S., Chase G. G. & Reneker D. H. (2008). Electrospun nanofibers from a porous hollow tube. *Polymer*, Vol. 49, No. 19, (September 2008), pp. 4226-29, ISSN 0032-3861
- Varesano A., Carletto R. A. & Mazzuchetti G. (2009). Experimental investigations on the multi-jet electrospinning process. *Journal of Materials Processing Technology*, Vol. 209, No. 11, (June 2009), pp. 5178-85, ISSN 0924-0136
- Varesano A., Rombaldoni F., Mazzuchetti G., Tonin C. & Comotto R. (2010). Multi-jet nozzle electrospinning on textile substrates: observations on process and nanofiber mat deposition. *Polymer International*, Vol. 59, No. 12, (December 2010), pp. 1606-15, ISSN 1097-0126
- Wang X., Niu H. T., Lin T. & Wang X. (2009). Needleless electrospinning of nanofibers with a conical wire coil. *Polymer Engineering & Science*, Vol. 49, No. 8, (August 2009), pp. 1582-86, ISSN 1548-2634
- Wang X., Niu H. T., Wang X. & Lin T. (2009). Large-scale electrospinning of polymer nanofibers using needleless nozzle. *Proceedings of the 38th Textile Research Symposium*, (3-5 September 2009), pp. 117-122

- Wu D., Huang X., Lai X., Sun D. & Lin L. (2010). High Throughput Tip-Less Electrospinning via a Circular Cylindrical Electrode. *Journal of Nanoscience and Nanotechnology*, Vol. 10, No. 7, (July 2010), pp. 4221-26, ISSN 1533-4899
- Yang E., Shi J. & Xue Y. (2010). Influence of electric field interference on double nozzles electrospinning. *Journal of Applied Polymer Science*, Vol. 116, No. 6, (June 2010), pp. 3688-92, ISSN 1097-4628
- Yarin A. L. & Zussman E. (2004). Upward needleless electrospinning of multiple nanofibers. *Polymer*, Vol. 45, No. 9, (April 2004), pp. 2977-80, ISSN 1548-2634



## **Nanofibers - Production, Properties and Functional Applications**

Edited by Dr. Tong Lin

ISBN 978-953-307-420-7

Hard cover, 458 pages

**Publisher** InTech

**Published online** 14, November, 2011

**Published in print edition** November, 2011

As an important one-dimensional nanomaterial, nanofibers have extremely high specific surface area because of their small diameters, and nanofiber membranes are highly porous with excellent pore interconnectivity. These unique characteristics plus the functionalities from the materials themselves impart nanofibers with a number of novel properties for advanced applications. This book is a compilation of contributions made by experts who specialize in nanofibers. It provides an up-to-date coverage of in nanofiber preparation, properties and functional applications. I am deeply appreciative of all the authors and have no doubt that their contribution will be a useful resource for anyone associated with the discipline of nanofibers.

### **How to reference**

In order to correctly reference this scholarly work, feel free to copy and paste the following:

Haitao Niu, Xungai Wang and Tong Lin (2011). Needleless Electrospinning: Developments and Performances, Nanofibers - Production, Properties and Functional Applications, Dr. Tong Lin (Ed.), ISBN: 978-953-307-420-7, InTech, Available from: <http://www.intechopen.com/books/nanofibers-production-properties-and-functional-applications/needleless-electrospinning-developments-and-performances>

# **INTECH**

open science | open minds

### **InTech Europe**

University Campus STeP Ri  
Slavka Krautzeka 83/A  
51000 Rijeka, Croatia  
Phone: +385 (51) 770 447  
Fax: +385 (51) 686 166  
[www.intechopen.com](http://www.intechopen.com)

### **InTech China**

Unit 405, Office Block, Hotel Equatorial Shanghai  
No.65, Yan An Road (West), Shanghai, 200040, China  
中国上海市延安西路65号上海国际贵都大饭店办公楼405单元  
Phone: +86-21-62489820  
Fax: +86-21-62489821

© 2011 The Author(s). Licensee IntechOpen. This is an open access article distributed under the terms of the [Creative Commons Attribution 3.0 License](#), which permits unrestricted use, distribution, and reproduction in any medium, provided the original work is properly cited.